Filament Depolymerization by Motor Molecules

Gernot A. Klein,[1] Karsten Kruse,[1] Gianaurelio Cuniberti,[1,2] and Frank Jülicher[1]

[1]*Max Planck Institute for the Physics of Complex Systems, D-01187 Dresden, Germany*

[2]*Institute for Theoretical Physics, University of Regensburg, D-93040 Regensburg, Germany*

(Received 9 August 2004; published 15 March 2005)

Motor proteins that specifically interact with the ends of cytoskeletal filaments can induce filament depolymerization. A phenomenological description of this process is presented. We show that under certain conditions motors dynamically accumulate at the filament ends. We compare simulations of two microscopic models to the phenomenological description. The depolymerization rate can exhibit maxima and dynamic instabilities as a function of the bulk motor density for processive depolymerization. We discuss our results in relation to experimental studies of Kin-13 family motor proteins.

DOI: 10.1103/PhysRevLett.94.108102 PACS numbers: 87.16.Nn, 02.50.Ey

Many active processes in cells are driven by highly specialized motor proteins which interact with filaments of the cytoskeleton. Important examples are cell locomotion, cell division, and the transport of organelles inside the cell [1]. Cytoskeletal filaments are linear aggregates of proteins, for example, actin and tubulin. Actin filaments and microtubules are dynamic and can change their lengths by addition and removal of subunits at the ends [1–3]. Filaments show a structural asymmetry, which provides a direction for motion and force generation of bound molecular motors. These proteins are able to transduce the chemical energy of a fuel which is adenosine triphosphate (ATP), to mechanical work while interacting with a filament [4,5].

In addition to generating forces along filaments, motors can also interact with filament ends where they may influence the polymerization rate and thus the filament length. Examples are provided by the members of the Kin-13 subfamily of kinesin motor proteins [6–8]. A particular example is the mitotic centromere-associated kinesin (MCAK) which regulates the length of microtubules during cell division [9]. In the course of cell division, the chromosome pairs are separated by the mitotic spindle. In this process, shortening microtubules generate forces pulling the chromosomes towards the opposing poles of the cell. MCAK is localized at the microtubule ends which interact with chromosomes [9] and it has been shown that it induces depolymerization of microtubules [7]. In vitro assays and single molecule studies have shown that MCAK accumulates at both ends of stabilized microtubules and induces depolymerization at a rate which depends on the bulk motor concentration, while at the same time MCAK molecules do not generate directed motion along microtubules [7].

In this Letter, we discuss the dynamics of motor molecules which induce the shortening of the ends of filaments to which they bind using both a phenomenological description and more microscopic models. For simplicity, we consider one filament end and use a semi-infinite geometry. The density of bound motors at a distance $x \geq 0$ from the depolymerizing filament end is denoted $\rho(x)$. Here, we use a reference frame in which the depolymerizing end is located at $x = 0$ for all times. Motors occur in the bulk solution at concentration c. They bind to and detach from filaments with rates $\omega_a c/\rho_{\max}$ and ω_d, respectively, where $\rho_{\max}$ is the maximal density of motors for which binding sites on the filament saturate. Bound motors diffuse along the filament with a diffusion coefficient D and may also exhibit a directed average motion with velocity v_0. Note that v_0 in general depends on the density of motors ρ [10–13]. The density profile along the filament then obeys

$$\partial_t \rho + \partial_x j = \omega_a c\left(1 - \frac{\rho}{\rho_{\max}}\right) - \omega_d \rho. \tag{1}$$

The current of motors is given by $j = -D\partial_x \rho - v\rho$. Here, $v = v_0 + v_d$ is the total velocity of motors with respect to the filament end, with $v_d \geq 0$ denoting the depolymerization velocity. It is related to the rate Ω of subunit removal from the end by $v_d = \Omega a/N$, where a is the size of a subunit and N the number of protofilaments in the filament.

We assume that the rate of filament depolymerization is regulated by motors bound to the filament end. Therefore, the rate of subunit removal is a function $\Omega(\rho_0)$ of the motor density $\rho_0 = \rho(x = 0)$ at the end. It is useful to systematically expand Ω in powers of ρ_0

$$\Omega(\rho_0) = \Omega_0 + \Omega_1 \rho_0 + \Omega_2 \rho_0^2 + \mathcal{O}(\rho_0^3). \tag{2}$$

Here, we have introduced the expansion coefficients Ω_i. The subunit removal rate in the absence of motors Ω_0 in general depends on buffer conditions. In situations where filaments are stabilized, $\Omega_0 = 0$. For motors which induce filament depolymerization, $\Omega_1 > 0$. Since the rate Ω saturates for large densities, typically $\Omega_2 < 0$.

The description is completed by specifying the boundary conditions at $x = 0$ and for $x \to \infty$. At $x = 0$ the current $j(x = 0)$ at the filament end equals the net rate J at which motors attach to the filament end. Since motors attached to the end induce depolymerization, the rate $J(\rho_0)$ is a function of the motor density ρ_0 at the end and also depends on

buffer conditions. Again, we express J by an expansion in powers of ρ_0:

$$J(\rho_0) = J_0 + J_1\rho_0 + J_2\rho_0^2 + \mathcal{O}(\rho_0^3). \quad (3)$$

Here, J_0 is the rate of direct motor attachments to the end. The coefficients J_1 and J_2 characterize how interactions between motors and the filament end influence the detachment rate of motors. If $v > 0$, motors typically detach from the end and thus $J < 0$.

Finally, for large x we require that the density ρ approaches the equilibrium value of the attachment-detachment dynamics

$$\rho_\infty = \frac{\omega_a c \rho_{\max}}{\omega_a c + \omega_d \rho_{\max}}. \quad (4)$$

If a motor bound to the end removes a filament subunit, it may fall off the filament with this subunit or it may stay bound to the filament. The tendency of a motor to stay attached while removing subunits can be described by its processivity. In our phenomenological description, we define the effective processivity

$$p_{\text{eff}} = 1 - \left| \frac{J(\rho_0) - J(0)}{\Omega(\rho_0) - \Omega(0)} \right|. \quad (5)$$

It differs from the processivity of an isolated motor due to collective effects resulting from interactions between motors at the end and thus depends on ρ_0. If $p_{\text{eff}} \leq 0$, more motors detach from the end than subunits and the motor-induced depolymerization is nonprocessive. However, if $0 < p_{\text{eff}} \leq 1$, a given motor can remove more than one subunit [14].

For simplicity, we ignore the density dependence of v_0. In this case, Eq. (1) approaches for large times t, a steady state given by $\rho = \rho_\infty + (\rho_0 - \rho_\infty)\exp[-x/\lambda]$. The characteristic length is

$$\lambda = \frac{2D}{v + [v^2 + 4D(\omega_a c/\rho_{\max} + \omega_d)]^{1/2}}. \quad (6)$$

The steady state value of ρ_0 is obtained by inserting this expression in Eq. (3). In the following, we consider the case where $v_d \gg |v_0|$ and the spontaneous velocity v_0 can be neglected. Indeed, experimental observations of MCAK show that $v_d \gg |v_0|$ [7]. Depending on parameters, motors either accumulate or deplete at the filament end, see Fig. 1. Accumulation at the end occurs for $\Omega_2 > \Omega_2^{(a)}$, where

$$\Omega_2^{(a)} = -\frac{\Omega_1 + J_2\rho_{\max}}{\rho_\infty} - \frac{\Omega_0 + J_1\rho_{\max}}{\rho_\infty^2} - \frac{J_0\rho_{\max}}{\rho_\infty^3}. \quad (7)$$

Motor accumulation can exhibit a reentrant behavior as a function of increasing bulk motor concentration; see Fig. 1.

Our phenomenological description reveals that motors can dynamically accumulate at the filament end even if their binding affinity to the end is not larger than in the bulk, $J_0 = 0$. In this process, motors which bind along the filament are subsequently captured by the retracting filament end. Dynamical accumulation of motors is a collective phenomenon and requires a sufficiently large effective processivity.

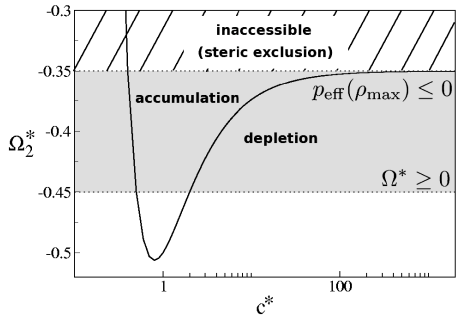

FIG. 1. Regimes of accumulation and depletion of motors at the shrinking filament end as a function of the coefficient $\Omega_2^* = \Omega_2\rho_{\max}/(D\omega_d)^{1/2}$ and the bulk motor concentration $c^* = \omega_a c/\omega_d\rho_{\max}$ for $J_0 = \Omega_0 = J_2 = 0$ and $J_1/(D\omega_d)^{1/2} = -0.1$, $\Omega_1/(D\omega_d)^{1/2} = 0.45$. Accumulation occurs above the solid line, depletion occurs below. The gray area indicates the region of physical interest. Above this area, $p_{\text{eff}}(\rho_{\max}) > 0$ which is forbidden by steric exclusion of particles. Below this area, filaments polymerize at high motor concentration.

In order to obtain a physical picture of the microscopic events which influence the effective processivity as a result of crowding, we extend discrete stochastic models for motor displacements along filaments [10–13] to capture subunit removal at the ends. Motors are represented by particles which occupy discrete binding sites indexed by $i = 1, 2, 3, \ldots$ arranged linearly on a filament which consists of a single proto-filament ($N = 1$); see Fig. 2. Here, $i = 1$ denotes the binding site at the filament end. Each site is either empty ($n_i = 0$) or occupied ($n_i = 1$). Particles move stochastically to neighboring empty sites with rate $\bar{\omega}_h$ in both directions. Here, we assume again that v_0 can be neglected as compared to v_d. In addition, particles attach to and detach from the lattice with rates $\bar{\omega}_a c$ and $\bar{\omega}_d$, respectively. The rates of particle attachment and detachment at the end site $i = 1$ differ from the bulk rates and are denoted $\bar{\Omega}_a c$ and $\bar{\Omega}_d$.

We first consider the situation where only one particle is present. If this particle is not bound at the end, the end is stable. If the particle is bound at $i = 1$, this subunit is

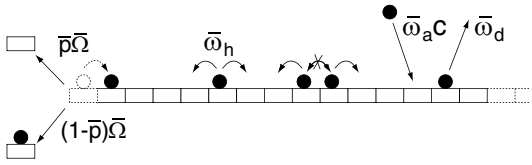

FIG. 2. Discrete model of motor-induced filament depolymerization. Motors attach to empty sites at rate $\bar{\omega}_a c$ and detach with rate $\bar{\omega}_d$. The hopping rate to free neighboring sites is $\bar{\omega}_h$. Occupied sites are removed from the end with rate $\bar{\Omega}$. With probability $\bar{p}$, the particle remains attached to the end when a subunit is removed.

removed from the filament with rate $\bar{\Omega}$. This process can occur in two different ways: (i) with probability $\bar{p}$ the particle stays bound to the new filament end after the first subunit is removed; (ii) with probability $1 - \bar{p}$ the particle detaches from the filament together with the removed subunit. If $\bar{p}$ is close to 1, a single particle is processive and can repeatedly remove subunits from the end without falling off.

Processive removal of a subunit requires simultaneous interaction of a motor with the end and the adjacent subunit. Therefore, this process is affected by the presence of other particles bound to the filament near the end. In particular, if site $i = 2$ is occupied while subunit $i = 1$ is removed, the new end site is already occupied and the particle at $i = 1$ cannot stay attached. We distinguish two cases with different behaviors in this situation. Model A describes the case where subunit removal by a motor requires an empty adjacent binding site, while model B corresponds to the case where the rate of subunit removal is independent of the occupation of the adjacent site. In model A, the probability per unit time to remove the end if $n_1 = 1$ is $\bar{\Omega}^A = \bar{\Omega}(1 - \bar{p}n_2)$. Here we assume that the processivity characterized by $\bar{p}$ is unaffected by the occupation of the neighboring site. Crowding at the end obstructs cutting and reduces the rate of subunit removal. In model B, an occupied adjacent site will reduce the processivity of a motor but does not affect the depolymerization rate, i.e., $\bar{\Omega}^B = \bar{\Omega}$.

We can represent the dynamics of the system by a master equation for the probability $P\{n_i, t\}$ to find a configuration of lattice occupation $(n_1, n_2, \ldots)$ at time t. This leads to expressions for the rate of change of average occupation numbers valid for $i \geq 2$:

$$\frac{d\langle n_i\rangle}{dt} = \bar{\omega}_h(\langle n_{i+1}\rangle - 2\langle n_i\rangle + \langle n_{i-1}\rangle) + \bar{\omega}_a c\langle 1 - n_i\rangle - \bar{\omega}_d\langle n_i\rangle + \langle \bar{\Omega}^{A,B} n_1(n_{i+1} - n_i)\rangle. \quad (8)$$

At the filament end, $i = 1$,

$$\frac{d\langle n_1\rangle}{dt} = \bar{\omega}_h\langle n_2 - n_1\rangle + \bar{\Omega}_a c\langle 1 - n_1\rangle - \bar{\Omega}_d\langle n_1\rangle - (1 - \bar{p})\bar{\Omega}\langle n_1(1 - n_2)\rangle. \quad (9)$$

Using a mean-field approximation, replacing two-point correlators $\langle n_i n_{i+1}\rangle$ by $\langle n_i\rangle\langle n_{i+1}\rangle$, we obtain from Eqs. (8) and (9) differential equations and boundary conditions identical to Eqs. (1)–(3) with $\rho(x = a(i-1)) = \langle n_i\rangle/a$. This procedure leads to explicit expressions for the values of the coefficients Ω_i and J_i introduced above. For both models A and B we find, using this approximation, $D = a^2\bar{\omega}_h$, $\Omega_1 = a\bar{\Omega}$, $J_0 = \bar{\Omega}_a c$, and $J_1 = -a(\bar{\Omega}_a c + \bar{\Omega}_d + (1 - \bar{p})\bar{\Omega})$. The nonlinear coefficients Ω_2 and J_2 are model dependent. In model A, $\Omega_2 = -a^2\bar{p}\,\bar{\Omega}$ and $J_2 = 0$ whereas for model B, $\Omega_2 = 0$ and $J_2 = -a^2\bar{p}\,\bar{\Omega}$. In both models all higher order coefficients Ω_n and J_n vanish.

Figure 3 displays the depolymerization velocity v_d obtained in the mean-field theory corresponding to model A as a function of the bulk monomer concentration c for different values of $\bar{p}$. For large c the velocity saturates at $v_d(\rho_{max})$, while it increases linearly for small c. For sufficiently large $\bar{p}$, the velocity v_d exhibits a maximum as a function of c. Increasing $\bar{p}$ further, a dynamic instability appears where two stable states with different v_d coexist within a range of c values. A third unstable state is indicated by a broken line. Results of stochastic simulations of model A are shown for comparison. Mean-field theory and stochastic simulation agree quantitatively except in the vicinity of the dynamic instability. Fluctuations conceal the dynamic instability present in mean-field theory. The inset to Fig. 3 shows the relative accumulation ρ_0/ρ_∞ of motors. For sufficiently large $\bar{p}$, motors accumulate as c is increased. We note that in model B, no dynamic accumulation of motors occurs and $\rho_0 < \rho_\infty$.

In summary, we have shown that a positive effective processivity p_{eff} of subunit removal is essential to achieve dynamic accumulation of motors at the filament end. This effective processivity is a collective effect and results from steric exclusion of motors bound near the end. The phenomenological description given by Eqs. (1)–(3) is general and valid irrespective of details of the mechanism of motor-induced subunit removal and of the structure of the depolymerizing filament end. We have restricted ourselves to effects corresponding to the lowest order terms in the expansions of Eqs. (2) and (3). While higher order terms could lead to additional effects, our simulations of

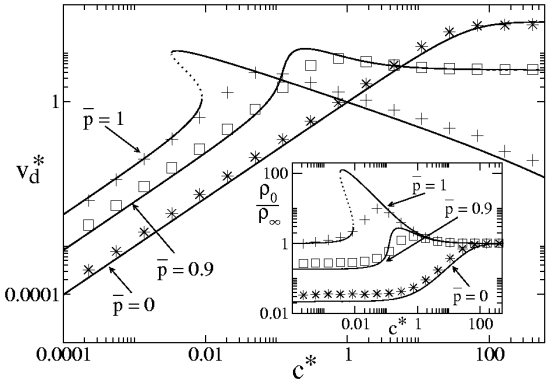

FIG. 3. The velocity $v_d^* = v_d/a(\bar{\omega}_h\bar{\omega}_d)^{1/2}$ of depolymerization as a function of the bulk motor concentration $c^* = \bar{\omega}_a c/\bar{\omega}_d$ obtained in simulations of model A for different values of the processivity $\bar{p} = 0$, 0.9, and 1 (symbols). For comparison the corresponding solutions of the phenomenological equations are displayed (lines). Inset: The accumulation of motors, characterized by the ratio ρ_0/ρ_∞ of motor density at the end and far from the end is shown as a function of c^* for the same situations. Parameter values are $\bar{\omega}_a = \bar{\Omega}_a$, $\bar{\omega}_d = \bar{\Omega}_d = 0.008\bar{\omega}_h$, and $\bar{\Omega} = 4\bar{\omega}_h$.

microscopic models indicate that these terms are unimportant (see Fig. 3). We have focussed on excluded volume effects at the filament end and have considered the case $v_0 = 0$ where some of these effects in the bulk disappear. For $v_0 \neq 0$, the interplay between bulk and end excluded volume effects could lead to new phenomena which will be subject of future work.

The stochastic models A and B provide a physical picture of the cooperativity and processivity of motors bound at the end of a single protofilament. Interactions between motors lead to different rates of subunit removal in the two models. In our stochastic simulations for a single protofilament, the dynamic instability of steady states which is found in the mean-field analysis is concealed by fluctuations. We expect that for larger numbers of protofilaments this effect of fluctuations is reduced. Therefore a signature of a dynamic instability could reappear for microtubule depolymerization leading to bistability and switch like changes of depolymerization velocities. In the mitotic spindle this instability could be relevant for chromosome oscillations, which have been observed [15].

Accumulation of motors at the filament end can occur as a result of three different mechanisms. Motors can accumulate by directly binding to the filament end if they have a higher affinity to the end than to subunits along the filament. This effect dominates if the total velocity $v = v_0 + v_d$ is small, $v^2 \ll 4D(\omega_a c/\rho_{max} + \omega_d)$. In this case, the localization length is given by the diffusion length during the attachment time $\lambda \simeq D^{1/2}(\omega_a c/\rho_{max} + \omega_d)^{-1/2}$. A second mechanism of accumulation is given by transport of motors to the end with velocity $v_0 \gg v_d$. In the third case, motors that bind along the filament are captured by the shortening end. This dynamic accumulation mechanism dominates for $v_0 \ll v_d$ and $v_d^2 \gg 4D(\omega_a c/\rho_{max} + \omega_d)$. The localization length is $\lambda \simeq D/v_d$. The first and last cases can lead to accumulation at both ends of a filament of finite length, while in the second case motors accumulate at one end only.

Our results can be related to experiments on members of the Kin-13 family of kinesins. The depolymerization velocity v_d as a function of bulk motor concentration has been measured for MCAK and it has been shown that MCAK accumulates at both ends [7]. The observed velocity v_d is consistent with both models A and B since it does not exclude the possibility of a maximal velocity for intermediate motor concentrations. Accumulation at the end suggests that a mechanism similar to model A is more likely to be at work. Indeed, experiments indicate that a collection of MCAK motors processively depolymerize microtubules [7] consistent with model A. Present data cannot rule out a mechanism akin to model B where motor accumulation is still possible if the affinity of motors to the filament end is high. In future experiments, model B could be ruled out if a maximum of the depolymerization velocity at intermediate motor concentration would be observed as suggested by our theory. The members XKCM1 and XKIF2 of the Kin-13 family can depolymerize microtubules with or without accumulation of motors at the end, depending on the conditions under which microtubules have been stabilized [6]. Furthermore, it has been suggested that processivity is reduced under conditions where motors do not accumulate [6]. Thus, stabilization of microtubules could influence the microscopic mechanisms of collective subunit removal by a change in the microtubule lattice structure, leading to reduced processivity $\bar{p}$ or a mechanism similar to model B.

The theory developed here is not restricted to motors of the Kin-13 family which interact with microtubules but applies in general to associated proteins which regulate the dynamics of filament ends. Actin depolymerization by actin-depolymerization factor/cofilin as well as the polymerization of actin by formin are further examples of such processes [16,17]. In addition to the conventional action of motor proteins, filament polymerization and depolymerization by processively acting end-binding proteins are expected to play a key role in cytoskeletal dynamics and self-organization.

We thank Stefan Diez and Joe Howard for fruitful discussions and stimulating collaborations. G. C. acknowledges support by the Volkswagen Stiftung.

[1] B. Alberts *et al.*, *Molecular Biology of the Cell* 4th ed., (Garland, New York, 2002).
[2] M. Dogterom and S. Leibler, Phys. Rev. Lett. **70**, 1347 (1993).
[3] C. Peskin, G. Odell, and G. Oster, Biophys. J. **65**, 316 (1993); C. Peskin and G. Oster, Biophys. J. **69**, 2268 (1995).
[4] J. Howard, *Mechanics of Motor Proteins & the Cytoskeleton* 4th ed., (Sinauer Associates, Sunderland, 2001).
[5] F. Jülicher. A. Ajdari, and J. Prost, Rev. Mod. Phys. **69**, 1269 (1997).
[6] A. Desai *et al.*, Cell **96**, 69 (1999).
[7] A. W. Hunter *et al.*, Mol. Cell **11**, 445 (2003).
[8] H. Bringmann *et al.*, Science **303**, 1519 (2004).
[9] L. Wordeman and T. J. Mitchison, J. Cell Biol. **128**, 95 (1995).
[10] R. Lipowsky, S. Klumpp, and T. M. Nieuwenhuizen, Phys. Rev. Lett. **87**, 108101 (2001).
[11] K. Kruse and K. Sekimoto, Phys. Rev. E **66**, 031904 (2002).
[12] A. Parmeggiani, T. Franosch, and E. Frey, Phys. Rev. Lett. **90**, 086601 (2003).
[13] S. Klumpp and R. Lipowsky, Europhys. Lett. **66**, 90 (2004).
[14] Note that the motor density at the end cannot exceed the maximal density, $\rho_0 \leq \rho_{max} = N/a$. Thus, the effective processivity vanishes for $\rho_0 = \rho_c$ with $\rho_c \leq \rho_{max}$.
[15] R. V. Skibbens *et al.*, J. Cell Biol. **122**, 859 (1993).
[16] D. Pruyne *et al.*, Science **297**, 612 (2002).
[17] I. Sagot *et al.*, Nat. Cell Biol. **4**, 626 (2002).